East Asian Journal on Applied Mathematics
doi: 10.4208/eajam.300418.300618

Vol. **8**, No. 3, pp. 598-610
August 2018

The Numerical Study of the Ground States of Spin-1 Bose-Einstein Condensates with Spin-Orbit-Coupling

Yongjun Yuan[1], Zhiguo Xu[2], Qinglin Tang[3] and Hanquan Wang[4,*]

[1]*Key Laboratory of HPC&SIP (MOE of China) and College of Mathematics and Statistics, Hunan Normal University, Changsha, Hunan 410081, P.R. China.*
[2]*College of Mathematics, Jilin University, Changchun, Jilin 130012, P.R. China.*
[3]*School of Mathematics, Sichuan University, Chengdu 610065, P.R. China.*
[4]*School of Statistics and Mathematics, Yunnan University of Finance and Economics, Kunming, Yunnan 650221, P.R. China.*

Received 30 April 2018; Accepted (in revised version) 30 June 2018.

Abstract. A projection gradient method for computing the ground state of the spin-orbit-coupled spin-1 Bose-Einstein condensate at extremely low temperatures is proposed. The continuous gradient flows are discretised by a second-order finite difference method in space and the Crank-Nicolson method in time. Our discretisation preserves the total mass conservation and the energy diminishing property. Numerical results show the efficiency of the method.

AMS subject classifications: 65M10, 78A48

Key words: Spin-orbit-coupled spin-1 Bose-Einstein condensate, projection gradient method, ground state, energy functional minimisation.

1. Introduction

Bose-Einstein condensate (BEC) is a state of matter of the dilute boson gas cooled close to absolute zero temperature. In these conditions, a large fraction of bosons occupy the lowest quantum state [26]. It was first observed in experiments in 1995 and became an ideal test ground for the experimental study of condensed matter phenomena. In particular, since the spin-orbit coupling (SOC) is ubiquitous in nature, the realisation of spin-orbit interaction in cold atomic gases is a hot topic nowadays [1, 9, 38, 39, 49]. Thus the spin-orbit coupling has been successfully induced in recent experiments in a neutral atomic Bose-Einstein condensates by dressing two atomic spin states with a pair of lasers [21–23]. These experiments triggered a strong activity in the area of spin-orbit-coupled cold atoms

*Corresponding author. *Email addresses:* `yuanyongjun0301@163.com` (Y. Yuan), `xuzg2014@jlu.edu.cn` (Z. Xu), `qinglin_tang@scu.edu.cn` (Q. Tang), `wang_hanquan@hotmail.com` (H. Wang)

and a number of exciting phenomena have been discovered [13,47]. The spin-1 BECs with isotropic spin-orbit coupling and rotation have been also studied — cf. Refs. [14,19,48]. It was found that SOC plays a crucial role in majorana fermions [45], spintronic devices [18], spin Hall effect [15] and topological insulators [10,27].

On the other hand, the creation of SOC in ultracold atomic gases attracted theoretical attention — cf. Refs. [6, 8, 11, 12, 21, 23, 29, 32, 35, 38, 47, 50]. In particular, BEC with various types of spin-orbit interaction has been considered in Refs. [20,24,34] and the spin-orbit-coupled BEC with distinct internal structures of bosons in Refs. [16, 17, 34, 36, 37]. Nevertheless, it is worth noting that although different couplings can generate non-trivial ground-state structures in spin-1/2, spin-1 and spin-2 BEC [4, 27, 33, 44, 46], there is no efficient numerical method to find such ground state solutions.

The projection gradient method (PGM), first used in nonlinear programming [30, 31], was later extended to functional minimisation problems with constraints [2, 25, 41, 42]. The key step in the method is the construction of a gradient flow projected into a feasible region or space. This approach has been recently combined with the conjugated gradient method [3]. Here we want to extend it onto energy functional minimisation with constraints and to use in the study of ground state solutions of the spin-orbit-coupled spin-1 BEC at extremely low temperatures. The method diminishes energy, conserves constraint during its implementation and evolves the continuous gradient flow to find the ground states.

This paper is organised as follows. In Section 2, we define the ground state solutions for spin-orbit coupled spin-1 BEC at very low temperatures and show that the ground state solutions satisfy the virial theorem. In Section 3, we use the projection gradient method to determine the ground state solutions of the spin-orbit-coupled spin-1 BEC and present two numerical methods for discretising the corresponding continuous gradient flows. In Section 4, we compare these numerical method and apply one of them to the ground state of the spin-orbit-coupled spin-1 BEC. Section 5 contains our conclusions and discussion.

2. Ground State of Spin-Orbit Coupled Spin-1 BEC

Let Ω be a bounded domain in $\mathbb{R}^d$. Using the physical Hamiltonian of the spin-orbit-coupled spin-1 BEC at very low temperature [11,33,43,46,47], we define the dimensionless energy functional of the spin-orbit-coupled spin-1 BEC by

$$
\begin{aligned}
&E(\phi_1,\phi_0,\phi_{-1})\\
=&\int_\Omega f(\phi_1,\bar{\phi}_1,\nabla\phi_1,\nabla\bar{\phi}_1,\cdots,\phi_{-1},\bar{\phi}_{-1},\nabla\phi_{-1},\nabla\bar{\phi}_{-1})d\mathbf{x}\\
=&\int_\Omega\Bigg\{\sum_{j=1,0,-1}\bar{\phi}_j h_d\phi_j+\frac{\beta_n}{2}\rho^2+\frac{\beta_s}{2}(\rho_1+\rho_0-\rho_{-1})\rho_1\\
&+\frac{\beta_s}{2}(\rho_1+\rho_{-1})\rho_0+\frac{\beta_s}{2}(\rho_0+\rho_{-1}-\rho_1)\rho_{-1}+\beta_s\left(\bar{\phi}_{-1}\phi_0^2\bar{\phi}_1+\phi_{-1}\bar{\phi}_0^2\phi_1\right)
\end{aligned}
$$

$$-\gamma\Big[(i\partial_x+\partial_y)\phi_0\bar{\phi}_1+(i\partial_x-\partial_y)\phi_1\bar{\phi}_0+(i\partial_x+\partial_y)\phi_{-1}\bar{\phi}_0+(i\partial_x-\partial_y)\phi_0\bar{\phi}_{-1}\Big]\Big\}d\mathbf{x}, \quad (2.1)$$

where γ is the spin-orbit coupling strength, $\phi_j=\phi_j(\mathbf{x})$, $j=1,0,-1$ are the wave functions, $\rho_j=|\phi_j|^2$ and $\rho:=\rho_1+\rho_0+\rho_{-1}$, $h_d:=-(1/2)\triangle+V$, and β_n, β_s are constants, respectively, related to the mean-field spin-independent and spin-exchange interactions. The wave functions are assumed to exponentially decay on $\mathbb{R}^d$ and vanish on the boundary $\partial\Omega$. Moreover, the wave functions ϕ_j, $j=1,0,-1$ are confined to the constraint

$$\int_\Omega g(\phi_1,\bar{\phi}_1,\phi_0,\bar{\phi}_0,\phi_{-1},\bar{\phi}_{-1})\,d\mathbf{x}=\int_\Omega\sum_{j=1,0,-1}|\phi_j(\mathbf{x})|^2\,d\mathbf{x}-1=0. \quad (2.2)$$

We are most interested in the ground state solution $\Phi^g=(\phi_1^g,\phi_0^g,\phi_{-1}^g)$ of the energy functional (2.1) under the constraint (2.2) — i.e. we consider the following problem:

Find $\Phi^g=(\phi_1^g,\phi_0^g,\phi_{-1}^g)\in S$ *such that*

$$E^g:=E(\phi_1^g,\phi_0^g,\phi_{-1}^g)=\min_{\Phi\in S}E(\Phi), \quad (2.3)$$

where

$$S:=\left\{(\Phi=(\phi_1,\phi_0,\phi_{-1})|\sum_{j=1,0,-1}\int_\Omega|\phi_j(\mathbf{x})|^2\,d\mathbf{x}=1\right\}. \quad (2.4)$$

Writing the functional $E(\phi_1,\phi_0,\phi_{-1})$ as

$$E(\phi_1,\phi_0,\phi_{-1})=E_{kin}+E_{pot}+E_{spin}+E_{soc},$$

with

$$E_{kin}=\frac{1}{2}\int_\Omega\left(\sum_{k=-1}^{1}|\nabla\phi_k|^2\right)d\mathbf{x},\quad E_{pot}=\int_\Omega\left(\sum_{k=-1}^{1}V_d(\mathbf{x})|\phi_k|^2\right)d\mathbf{x},$$
$$E_{spin}=\int_\Omega\Big\{\sum_{j=1,0,-1}\frac{\beta_n}{2}\rho^2+\frac{\beta_s}{2}(\rho_1+\rho_0-\rho_{-1})\rho_1+\frac{\beta_s}{2}(\rho_1+\rho_{-1})\rho_0$$
$$+\frac{\beta_s}{2}(\rho_0+\rho_{-1}-\rho_1)\rho_{-1}+\beta_s\left(\bar{\phi}_{-1}\phi_0^2\bar{\phi}_1+\phi_{-1}\bar{\phi}_0^2\phi_1\right)\Big\}\,d\mathbf{x},$$

and

$$E_{soc}=-\gamma\int_\Omega\big[(i\partial_x+\partial_y)\phi_0\bar{\phi}_1+(i\partial_x-\partial_y)\phi_1\bar{\phi}_0$$
$$+(i\partial_x+\partial_y)\phi_{-1}\bar{\phi}_0+(i\partial_x-\partial_y)\phi_0\bar{\phi}_{-1}\big]\,d\mathbf{x},$$

we can describe the ground state solutions by the following virial theorem.

Theorem 2.1. *If* $\mathbf{\Phi}^g = \left(\phi_1^g, \phi_0^g, \phi_{-1}^g\right)$ *is the exact ground state solution of* (2.1)*, then*

$$2E_{skin}(\mathbf{\Phi}^g) - 2E_{pot}(\mathbf{\Phi}^g) + dE_{spin}(\mathbf{\Phi}^g) + E_{soc}(\mathbf{\Phi}^g) = 0. \tag{2.5}$$

Proof. Let $d = 1,2,3$. Introducing trial functions $\phi_k^0(\mathbf{x})$, $k = 1,0,-1$ by

$$\phi_k^0(\mathbf{x}) = (1+\epsilon)^{d/2}\phi_k^g\left((1+\epsilon)\mathbf{x}\right),$$

we write the new evaluation of $E\left(\Phi^0\right)$ as

$$\begin{aligned} E(\epsilon) \equiv E\left(\Phi^0\right) &= E\left(\phi_1^0(\mathbf{x}), \phi_0^0(\mathbf{x}), \phi_{-1}^0(\mathbf{x})\right) \\ &= (1+\epsilon)^2 E_{kin}(\mathbf{\Phi}^g) + \frac{1}{(1+\epsilon)^2}E_{pot}(\mathbf{\Phi}^g) \\ &\quad + (1+\epsilon)^d E_{spin}(\mathbf{\Phi}^g) + (1+\epsilon)E_{soc}(\mathbf{\Phi}^g). \end{aligned} \tag{2.6}$$

Since $\mathbf{\Phi}^g = \left(\phi_1^g(\mathbf{x}), \phi_0^g(\mathbf{x}), \phi_{-1}^g(\mathbf{x})\right)$ is the exact ground state solution, the function $E(\epsilon)$ has a minimum at $\epsilon = 0$, hence

$$\frac{\partial E(\epsilon)}{\partial \epsilon}\Big|_{\epsilon=0} = 0. \tag{2.7}$$

Substituting (2.6) into the Eq. (2.7) leads to the relation (2.5). □

3. Projection Gradient Method for Ground States

In this section, we use the PGM in order to find the ground states of the spin-orbit coupled spin-1 BECs, which is the global minima of the energy functional (2.1) under the constraint (2.2). The construction of PGM consists in three steps:

1. Write the minimisation problem corresponding the given energy functional and constrain conditions.
2. Define a projected continuous gradient flows (CGFs) with Lagrangian multipliers associated with constrain conditions.
3. Discretise the CGFs and apply a conservative numerical methods — e.g. a finite difference or a finite element method.

For more details, we refer the reader to [41,42].

To find the minimiser of (2.3), we consider the following CGFs:

$$\begin{aligned} \partial_t \phi_1 &= -\frac{\partial f}{\partial \bar{\phi}_1} + \mathrm{div}\left(\frac{\partial f}{\partial \nabla \bar{\phi}_1}\right) + \lambda \frac{\partial g}{\partial \bar{\phi}_1} \\ &= \left(\frac{1}{2}\Delta - V - \beta_n \rho\right)\phi_1 - \beta_s(\rho_1 + \rho_0 - \rho_{-1})\phi_1 - \beta_s \bar{\phi}_{-1}\phi_0^2 \end{aligned}$$

$$+\gamma(i\partial_x+\partial_y)\phi_0+\lambda\phi_1, \tag{3.1}$$

$$\begin{aligned}\partial_t\phi_0&=-\frac{\partial f}{\partial\bar{\phi}_0}+\mathrm{div}\left(\frac{\partial f}{\partial\nabla\bar{\phi}_0}\right)+\lambda\frac{\partial g}{\partial\bar{\phi}_0}\\&=\left(\frac{1}{2}\Delta-V-\beta_n\rho\right)\phi_0-\beta_s(\rho_1+\rho_{-1})\phi_0-2\beta_s\phi_1\phi_{-1}\bar{\phi}_0\\&\quad+\gamma(i\partial_x-\partial_y)\phi_1+\gamma(i\partial_x+\partial_y)\phi_{-1}+\lambda\phi_0,\end{aligned} \tag{3.2}$$

$$\begin{aligned}\partial_t\phi_{-1}&=-\frac{\partial f}{\partial\bar{\phi}_{-1}}+\mathrm{div}\left(\frac{\partial f}{\partial\nabla\bar{\phi}_{-1}}\right)+\lambda\frac{\partial g}{\partial\bar{\phi}_{-1}}\\&=\left(\frac{1}{2}\Delta-V-\beta_n\rho\right)\phi_{-1}-\beta_s(\rho_0+\rho_{-1}-\rho_1)\psi_{-1}-\beta_s\bar{\phi}_1\phi_0^2\\&\quad+\gamma(i\partial_x-\partial_y)\phi_0+\lambda\phi_{-1},\end{aligned} \tag{3.3}$$

with the initial conditions

$$\phi_1(\mathbf{x},t=0)=\phi_1^0(\mathbf{x}),\ \ \phi_0(\mathbf{x},t=0)=\phi_0^0(\mathbf{x}),\ \ \phi_{-1}(\mathbf{x},t=0)=\phi_{-1}^0(\mathbf{x}), \tag{3.4}$$

and the Dirichlet zero boundary condition. We note that λ is determined by the equation

$$\begin{aligned}\lambda=&\int_\Omega\Big\{\sum_{j=1,0,-1}\bar{\phi}_jh_d\phi_j+\beta_n\rho^2+\beta_s(\rho_1+\rho_0-\rho_{-1})\rho_1\\&+\beta_s(\rho_1+\rho_{-1})\rho_0+\beta_s(\rho_0+\rho_{-1}-\rho_1)\rho_{-1}\\&+2\lambda_s\left(\bar{\phi}_{-1}\phi_0^2\bar{\phi}_1+\phi_{-1}(\bar{\phi}_0)^2\phi_1\right)-\gamma\big[(i\partial_x+\partial_y)\phi_0\bar{\phi}_1+(i\partial_x-\partial_y)\phi_1\bar{\phi}_0\\&+(i\partial_x+\partial_y)\phi_{-1}\bar{\phi}_0+(i\partial_x-\partial_y)\phi_0\bar{\phi}_{-1}\big]\Big\}d\mathbf{x}\Big/\int_\Omega\left(|\phi_1|^2+|\phi_0|^2+|\phi_{-1}|^2\right)d\mathbf{x}.\end{aligned}$$

The following theorem plays an important role in computing the ground states of the spin-orbit-coupled spin-1 BECs.

Theorem 3.1. *If CGFs* (3.1)-(3.3) *is provided with Dirichlet zero boundary conditions and the initial conditions* (3.4)*, then the relations*

$$\begin{aligned}&(1)\quad\sum_{j=1,0,-1}||\phi_j(\mathbf{x},t)||^2=\sum_{j=1,0,-1}||\phi_j^0(\mathbf{x})||^2,\\&(2)\quad\frac{\partial}{dt}E(\phi_1(\mathbf{x},t),\phi_0(\mathbf{x},t),\phi_{-1}(\mathbf{x},t))\le 0,\end{aligned}$$

hold.

The proof of this result is analogous to the proof of Lemma 3.1 in [41].

Thus CGFs (3.1)-(3.3) has norm conservation and energy diminishing properties. The first one guaranties that the gradient flows (3.1)-(3.3) always belong to the corresponding feasible space (2.4). Moreover, if t tends to ∞, the vector $(\phi_1(\mathbf{x},t),\phi_0(\mathbf{x},t),\phi_{-1}(\mathbf{x},t))$

approaches a local minimum of the energy functional $E\left(\phi_1(\mathbf{x},t),\phi_0(\mathbf{x},t),\phi_{-1}(\mathbf{x},t)\right)$, and for suitable initial data $\left(\phi_1(\mathbf{x},0),\phi_0(\mathbf{x},0),\ \phi_{-1}(\mathbf{x},0)\right)$ one has

$$\phi_j(\mathbf{x},t)\to\phi_j^g(\mathbf{x}),\quad j=1,0,-1\quad\text{as}\quad t\to\infty. \tag{3.5}$$

Let us now consider two numerical methods for the CGFs (3.1)-(3.3). The first one — viz. the PGM, allows us the direct discretisation of the CGFs (3.1)-(3.3) by the Crank-Nicolson scheme in time. Thus

$$\begin{aligned}
\frac{\phi_1^{n+1}-\phi_1^n}{\triangle t}=&\left(\frac{1}{2}\Delta-V-\beta_n\rho^{n+1/2}\right)\phi_1^{n+1/2}\\
&-\beta_s(\rho_1^{n+1/2}+\rho_0^{n+1/2}-\rho_{-1}^{n+1/2})\phi_1^{n+1/2}-\beta_s\bar{\phi}_{-1}^{n+1/2}\left(\phi_0^{n+1/2}\right)^2\\
&+\gamma(i\partial_x+\partial_y)\phi_0^{n+1/2}+\lambda^{n+1/2}\phi_1^{n+1/2}, &(3.6)\\
\frac{\phi_0^{n+1}-\phi_0^n}{\triangle t}=&\left(\frac{1}{2}\Delta-V-\beta_n\rho^{n+1/2}\right)\phi_0^{n+1/2}-\beta_s(\rho_1^{n+1/2}+\rho_{-1}^{n+1/2})\phi_0^{n+1/2}\\
&-2\beta_s\phi_1^{n+1/2}\phi_{-1}^{n+1/2}\bar{\phi}_0^{n+1/2}+\gamma(i\partial_x-\partial_y)\phi_1^{n+1/2}\\
&+\gamma(i\partial_x+\partial_y)\phi_{-1}^{n+1/2}+\lambda^{n+1/2}\phi_0^{n+1/2}, &(3.7)\\
\frac{\phi_{-1}^{n+1}-\phi_{-1}^n}{\triangle t}=&\left(\frac{1}{2}\Delta-V-\beta_n\rho^{n+1/2}\right)\phi_{-1}^{n+1/2}\\
&-\beta_s(\rho_0^{n+1/2}+\rho_{-1}^{n+1/2}-\rho_1^{n+1/2})\psi_{-1}^{n+1/2}-\beta_s\bar{\phi}_1^{n+1/2}\left(\phi_0^{n+1/2}\right)^2\\
&+\gamma(i\partial_x-\partial_y)\phi_0^{n+1/2}+\lambda^{n+1/2}\phi_{-1}^{n+1/2}, &(3.8)
\end{aligned}$$

where $\phi_j^n=\phi(\mathbf{x},t_n)$, $j=1,0,-1$ for all $t_n=n\triangle t$, $\rho_j^n=|\phi_j^n|^2$, $\phi_j^{n+1/2}=(\phi_j^n+\phi_j^{n+1})/2$ and $\rho_j^{n+1/2}=(\rho_j^n+\rho_j^{n+1})/2$. Besides, the integral term $\lambda^{n+1/2}$ in (3.6)-(3.8) is determined as

$$\begin{aligned}
\lambda^{n+1/2}=&\int_\Omega\Bigg\{\sum_{j=1,0,-1}\bar{\phi}_j^{n+1/2}h_d\phi_j^{n+1/2}+\beta_n\left(\rho^{n+1/2}\right)^2\\
&+\beta_s(\rho_1^{n+1/2}+\rho_0^{n+1/2}-\rho_{-1}^{n+1/2})\rho_1^{n+1/2}\\
&+\beta_s(\rho_1^{n+1/2}+\rho_{-1}^{n+1/2})\rho_0^{n+1/2}+\beta_s(\rho_0^{n+1/2}+\rho_{-1}^{n+1/2}-\rho_1^{n+1/2})\rho_{-1}^{n+1/2}\\
&+2\lambda_s\left(\bar{\phi}_{-1}^{n+1/2}\left(\phi_0^{n+1/2}\right)^2\bar{\phi}_1^{n+1/2}+\phi_{-1}^{n+1/2}\left(\bar{\phi}_0^{n+1/2}\right)^2\phi_1^{n+1/2}\right)\\
&-\gamma\Big[(i\partial_x+\partial_y)\phi_0^{n+1/2}\bar{\phi}_1^{n+1/2}+(i\partial_x-\partial_y)\phi_1^{n+1/2}\bar{\phi}_0^{n+1/2}+(i\partial_x+\partial_y)\phi_{-1}^{n+1/2}\bar{\phi}_0^{n+1/2}\\
&+(i\partial_x-\partial_y)\phi_0^{n+1/2}\bar{\phi}_{-1}^{n+1/2}\Big]\Bigg\}d\mathbf{x}\Bigg/\int_\Omega\left(|\phi_1^{n+1/2}|^2+|\phi_0^{n+1/2}|^2+|\phi_{-1}^{n+1/2}|^2\right)d\mathbf{x}. \qquad (3.9)
\end{aligned}$$

The semi-discretised system (3.6)-(3.8) can be discretised in space by the central finite difference method and the integral term $\lambda^{1/2}$ in (3.9) by the composite trapezoidal rule.

We also can solve the CGFs (3.1)-(3.3) by the gradient flow with discrete normalisation (GFDN) — cf. [5]. It can be described as follows:

1. Find the approximate values $\phi_j(\mathbf{x},t_{n+1}^-)$, $j=1,0,-1$ for the gradient flow from t_n to t_{n+1} from the equations

$$\begin{aligned}\partial_t\phi_1=&\left(\frac{1}{2}\Delta-V-\beta_n\rho\right)\phi_1-\beta_s(\rho_1+\rho_0-\rho_{-1})\phi_1-\beta_s\bar{\phi}_{-1}\phi_0^2\\&+\gamma(i\partial_x+\partial_y)\phi_0, \qquad (3.10)\\ \partial_t\phi_0=&\left(\frac{1}{2}\Delta-V-\beta_n\rho\right)\phi_0-\beta_s(\rho_1+\rho_{-1})\phi_0-2\beta_s\phi_1\phi_{-1}\bar{\phi}_0\\&+\gamma(i\partial_x-\partial_y)\phi_1+\gamma(i\partial_x+\partial_y)\phi_{-1}, \qquad (3.11)\\ \partial_t\phi_{-1}=&\left(\frac{1}{2}\Delta-V-\beta_n\rho\right)\phi_{-1}-\beta_s(\rho_0+\rho_{-1}-\rho_1)\psi_{-1}-\beta_s\bar{\phi}_1\phi_0^2\\&+\gamma(i\partial_x-\partial_y)\phi_0. \qquad (3.12)\end{aligned}$$

2. Project the approximate solution at time t_{n+1} into feasible space S with manual discrete normalisation

$$\phi_j(\mathbf{x},t_{n+1})=\frac{\phi_j(\mathbf{x},t_{n+1}^-)}{\sqrt{||\phi_1(\mathbf{x},t_{n+1}^-)||^2+||\phi_0(\mathbf{x},t_{n+1}^-)||^2+||\phi_{-1}(\mathbf{x},t_{n+1}^-)||^2}}, \qquad (3.13)$$

   where
$$||\phi_j(\mathbf{x},t_{n+1}^-)||^2=\int_\Omega|\phi_j(\mathbf{x},t_{n+1}^-)|^2d\mathbf{x}.$$

   We note that the GFDN can be considered as first-order time splitting method for solving the CGFs (3.1)-(3.3) from t_n to t_{n+1}.

In the next section, we discretise the Eqs. (3.6)-(3.8) or (3.10)-(3.12) by a second-order finite difference method in space and by the Crank-Nicolson method in time. The equations obtained are solved by standard iterative methods, the details of which can be found in Refs. [7,41,42].

The main difference in the above methods is that the PGM does not require a manual projection step. Therefore, from computational point of view it is easier to implement the PGM and to use it in the ground state simulation of energy functionals with multiple constrain conditions, which is not always possible with the GFDN.

4. Numerical Results

In this section, we use the PGM to determine the ground state solution of a spin-orbit-coupled spin-1 BEC. The computation domain $\Omega=(-12,12)^d$, $d=1,2$ is covered by $N=129$ equidistant grid points in each of x- and y-directions. In 2-dimensional case, the harmonic trap potential function is $V(\mathbf{x})=(x^2+y^2)/2$ and the initial data for the flows are

$$\phi_j(x,y,t=0)=\frac{1}{\sqrt{6\pi}}e^{-\frac{x^2+y^2}{2}}, \quad j=1,0,-1.$$

4.1. Efficiency test

Let us compare the numerical results obtained by the discretisation methods above. Note that the PGM requires solving a partial differential equation with an integral term, while for the GFDN this operation can be replaced by the normalisation at each numerical time step.

We choose $\beta_n = 871.6\times M$, $\beta_s = -17.48\times M$ and $\gamma = 0$ in (2.1) in one-dimensional and two-dimensional situations. Tables 1 and 2 show the computed energy of ground state and the CPU cost for PGM and GFDN, respectively. We observe that for small M the energies of the ground states found by PGM and GFDN are close to each other, but for larger M the PGM provides lower energy values. Moreover, for all parameters M tested, the CPU time for PGM is comparable or smaller than for GFDN. Hence, the PGM is more efficient.

Table 1: Numerical comparison of the discretisation methods for different parameters M in 1D-case, $\beta_n = 871.6 \times M$, $\beta_s = -17.48 \times M$.

	PGM		GFDN	
M	Energy	CPU time	Energy	CPU time
1	7.6760	3.51	7.6765	3.6972
5	22.3053	2.496	22.3398	2.3556
10	35.2219	2.106	35.4459	2.2152
20	54.8234	1.95	56.2557	2.0904
50	99.4696	2.1372	103.6135	2.3281

Table 2: Numerical comparison of the discretisation methods for different parameters M in 2D-case, $\beta_n = 871.6 \times M$, $\beta_s = -17.48 \times M$.

	PGM		GFDN	
M	Energy	CPU time	Energy	CPU time
1	3.6750	1131.9276	3.6749	1195.108
5	7.8883	556.5804	7.8884	746.964
10	11.0859	448.5809	11.0858	597.7646
20	15.6234	390.3613	15.6239	475.625
50	23.4159	333.2649	24.6875	415.0563

4.2. Ground states for spin-orbit coupled spin-1 BECs

Now we calculate the ground state of spin-orbit coupled spin-1 BEC by the PGM. In order to show the properties of the ground states and illustrate Theorem 2.1, we choose the parameters $\beta_n = 871.6 \times M$, $\beta_s = 17.48 \times M$ and $\gamma = 1$ in (2.1) and define the residual of (2.5) by

$$Res_V = 2E_{kin} - 2E_{pot} + 2E_{spin} + E_{soc}.$$

Table 3: Numerical tests for Theorem 2.1. $\beta_n = 871.6\times M$, $\beta_s = 17.48\times M$ and $\gamma=1$.

M	E_{kin}	E_{har}	E_{spin}	E_{soc}	Res_V
1	1.0525	1.7988	1.7031	-1.9504	-0.0367
5	0.9977	3.9226	3.8685	-1.9313	-0.0442
10	0.9707	5.5270	5.4839	-1.9150	-0.0596
20	0.9583	7.8005	7.7657	-1.9109	-0.0638
100	0.9306	17.4230	17.3823	-1.8583	-0.0785

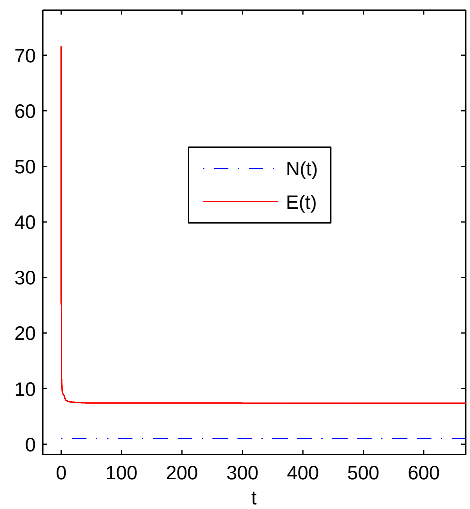

Figure 1: Norm conservation and energy diminishing property for ground state solutions of the spin-orbit coupled spin-1 BECs when the CGFs are evolved by the PGM.

Table 3 demonstrates that the ground state solution of spin-orbit coupled spin-1 BEC satisfies Theorem 2.1 for M from 1 to 100. Moreover, Fig. 1 shows that for the gradient flow (3.6)-(3.8), the total mass

$$N(t) := \int_\Omega \sum_{j=1,0,-1} |\phi_j|^2\, dxdy,$$

of the approximate solutions is conserved and the corresponding total energy $E(t) := E(\phi_1(x,y,t),\phi_0(x,y,t),\phi_{-1}(x,y,t))$ decreases when t increases. Thus these numerical results agree with Theorem 3.1, so that the ground state solution of the spin-orbit coupled spin-1 BEC satisfies the virial theorem. Next we choose $\beta_n = 871.6$, $\beta_s = 17.48$ and different spin-orbit-coupling parameters γ to simulate the stripe pattern ground states — cf. Fig. 2. Note that the stripe pattern ground state solutions of the spin-1 BECs obtained for the increasing parameter γ are consistent with observation [43].

Finally we take $\beta_n = 871.6$ and $\beta_s = -17.48$ with different spin-orbit-coupling parameters γ — cf. Fig. 3 and note that the square-lattice pattern of the ground state solutions of spin-1 BECs are obtained for the increasing spin-orbit coupling strength γ, which agrees with the conjecture in [46].

Figs. 2-3 show that the two patterns of the ground states of spin-orbit coupled spin-1 BECs are mainly determined by the sign of the interaction parameter β_s, similar to the case of the general spin-1 BECs. It is well known that for $\beta_s > 0$ the ground states of spin-1 BECs are antiferromagnetic and they are ferromagnetic if $\beta_s < 0$ — cf. Ref. [17].

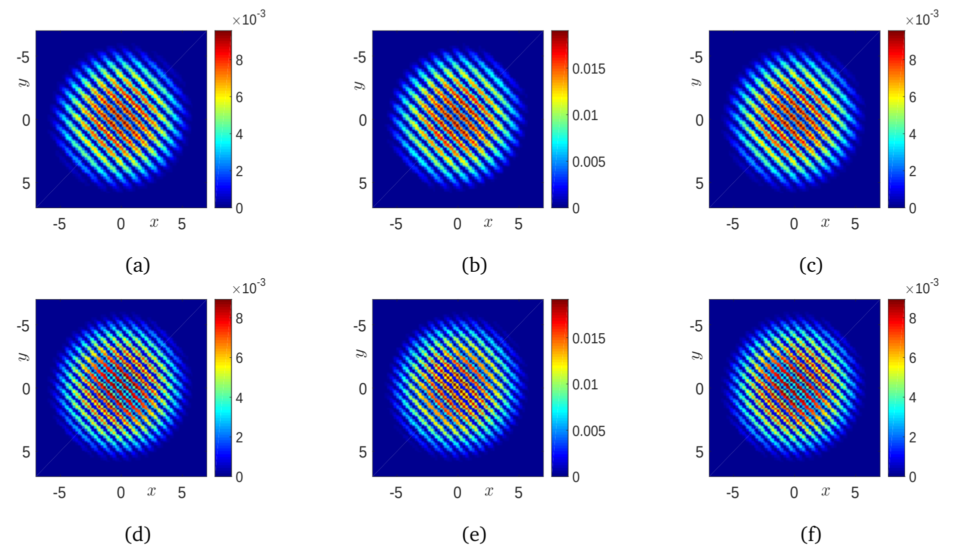

Figure 2: Density image of ground state solutions for the spin-1 BECs with $\beta_n = 871.6$, $\beta_s = 17.48$. First row: $\gamma = 3$. Second row: $\gamma = 4$. (a)(d): $|\phi_1^g(x,y)|^2$; (b)(e): $|\phi_0^g(x,y)|^2$; (c)(f): $|\phi_{-1}^g(x,y)|^2$.

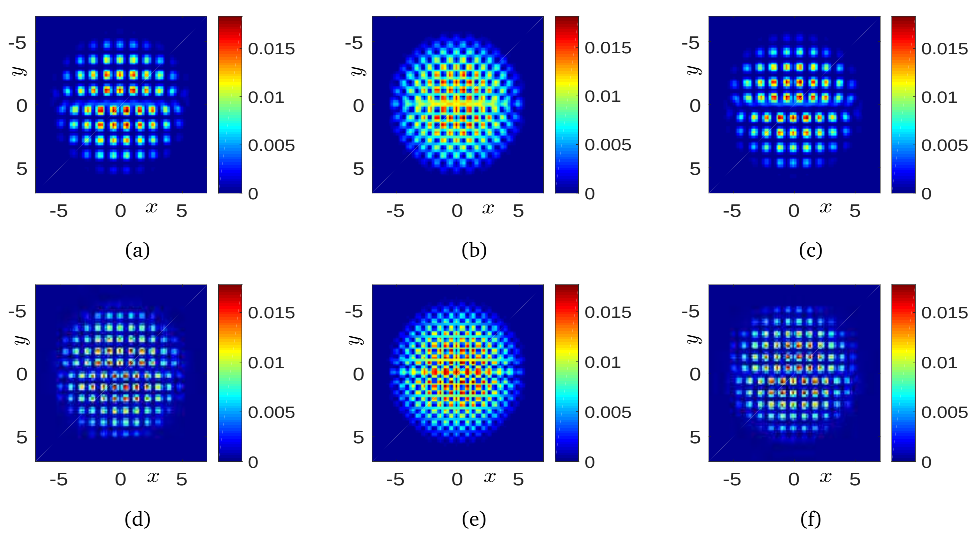

Figure 3: Density image of ground state solutions for the spin-1 BECs with $\beta_n = 871.6$, $\beta_s = -17.48$. First row: $\gamma = 3$. Second Row: $\gamma = 4$. (a)(d): $|\phi_1^g(x,y)|^2$; (b)(e): $|\phi_0^g(x,y)|^2$; (c)(f): $|\phi_{-1}^g(x,y)|^2$.

5. Conclusions

We proposed a projection gradient method for computing the ground state of spin-orbit-coupled spin-1 Bose-Einstein condensates, which is, in a sense, an energy functional minimisation under one constraint. It is shown that this method has the property of energy diminishing and is constraint conservative if the continuous gradient flows are evolved to find the ground states of spin-orbit-coupled spin-1 BECs. It is used for computing the ground state solutions of the spin-orbit-coupled spin-1 BECs with different parameters. Interesting physical phenomena, such as the stripe-pattern and the square-lattice pattern of ground states are observed. The method can be extended to the ground state solutions of spin-orbit-coupled spin-2 Bose-Einstein condensates [16]. This will be done elsewhere.

Acknowledgments

We were supported in part by the Natural Science Foundation of China: YY by Grant No. 11601148, HW by Grant No. 91430103, and ZX by Grant No. 11501242. Moreover, QT was partially supported by the Fundamental Research Fund for the Central Universities and ZX by the Science and Technology Development Project(20170520055JH) and the Scientific Research Project of the Education Department of Jilin Province (JJKH20160398KJ).

References

[1] B. M. Anderson, G. Juzeliūnas, V. M. Galitski and I. B. Spielman, *Synthetic 3D spin-orbit coupling*, Phys. Rev. Lett. **108**, 235301 (2012).

[2] F. Alouges, *A new algorithm for computing liquid crystal stable configurations: the harmonic mapping case*, SIAM J. Numer. Anal. **34**, 1708-1726 (1997).

[3] X. Antoine, Q. Tang and Y. Zhang, *A preconditioned conjugated gradient method for computing fround states of rotating dipolar Bose-Einstein Condensates via kernel truncation method for dipole-dipole interaction evaluation*, Commun. Comput. Phys. **24**, 966-988 (2018).

[4] W. Bao and Y. Cai, *Mathematical models and numerical methods for spinor Bose-Einstein condensates*, Commun. Comput. Phys. **24**, 899-965 (2018).

[5] W. Bao and Q. Du, *Computing the ground state solution of Bose-Einstein condensates by a normalized gradient flow*, SIAM J. Sci. Comput. **25**, 1674-1697 (2004).

[6] W. Bao and Y. Cai, *Ground state and dynamics of spin-orbit-coupled Bose-Einstein Condensates*, SIAM J. Appl. Math. **75**, 492-517 (2015).

[7] W. Bao and H. Wang, *A mass and magnetization conservative and energy diminishing numerical method for computing ground state of spin-1 Bose-Einstein condensates*, SIAM J. Numer. Anal. **45**, 2177-2200 (2007).

[8] Y. Chen and M. Xie, *Spin-orbit-coupled Bose-Einstein condensates in a circular box*, Eur. Phys. J. D **69**, 138 (2015).

[9] V. Galitski and I. B. Spielman, *Spin-orbit coupling in quantum gases*, Nature **494**, 49-54 (2013).

[10] M. Z. Hasan and C. L. Kane, *Colloquium: Topological insulators*, Rev. Mod. Phys. **82**, 3045-3067 (2010).

[11] T. Ho and S. Zhang, *Bose-Einstein condensates with spin-orbit interaction*, Phys. Rev. Lett. **107**, 150403 (2011) .

[12] H. Hu, B. Ramachandhran, H. Pu, and X. Liu, *Spin-orbit coupled weakly interacting Bose-Einstein condensates in harmonic traps*, Phys. Rev. Lett. **108**, 010402 (2012).
[13] C. Hamner, C. Qu, Y. Zhang, J. Chang, M. Gong, C. Zhang and P. Engels, *Dicke-type phase transition in a spin-orbit-coupled Bose-Einstein condensate*, Nat. Commun. **5**, 4023 (2014).
[14] A.C. Ji, W.M. Liu, J.L. Song and F. Zhou, *Dynamical creation of fractionalized vortices and vortex lattices*, Phys. Rev. Lett. **101**, 010402 (2008).
[15] Y. K. Kato, R. C. Myers, A. C. Gossard and D. D. Awschalom, *Observatioin of the spin Hall effect in semiconductors*, Science **306**, 1910-1913 (2004).
[16] T. Kawakami, T. Mizushima and K. Machida, *Textures of spin-orbit coupled F=2 spinor Bose Einstein condensates*, Phys. Rev. A **84**, 011607(R) (2011).
[17] Y. Kawaguchi and M. Ueda, *Spinor Bose-Einstein condensates*, Phys. Rep. **520**, 253-381 (2012).
[18] J. D. Koralek, C. P. Weber, J. Orenstein, B. A. Bernevig, S. C. Zhang, S. Mack and D. D. Awschalom, *Emergence of the persistent spin helix in semiconductor quantum wells*, Nature, **458**, 610-613 (2009).
[19] R. Liao, Y.X. Yu and W.M. Liu, *Tuning the tricritical point with spin-orbit coupling in polarized Fermionic condensates*, Phys. Rev. Lett. **108**, 080406 (2012).
[20] Y. Li, G.I. Martone1 and S. Stringari, *Bose-Einstein condensation with spin-orbit coupling*, Annual Review of Cold Atoms and Molecules, Vol. **3** (World Scientific, 2015), Chap. 5, 201-250 (2015).
[21] Y.J. Lin, R.L. Compton, A.R. Perry, W.D. Phillips, J.V. Porto and I.B. Spielman, *Bose-Einstein condensates in a uniform light-induced vector potential*, Phys. Rev. Lett. **102**, 130401 (2009).
[22] Y.J. Lin, K. Jiménez-Garcia and I.B. Spielman, *A spin-orbit coupled Bose-Einstein condensate*, Nature, **471**, 83-86 (2011).
[23] Y.J. Lin, R.L. Compton, K. Jiméz-Garcia, J.V. Porto and I.B. Spielman, *Synthetic magnetic fields for ultracold neutral atoms*, Nature **462**, 628-632 (2009).
[24] T. Ozawa and G. Baym, *Ground-state phases of ultracold bosons with Rashba-Dresselhaus spin-orbit coupling*, Phys. Rev. A **85**, 013612 (2012).
[25] S. Osher and R. Fedkiw, *Level Set Methods and Dynamic Implicit Surfaces*, Springer-Verlag (2003).
[26] L. Pitaevskii and S. Stringari, *Bose-Einstein condensation*, Clarendon Press (2003).
[27] X.L. Qi and S.C. Zhang, *Topological insulators and superconductors*, Rev. Mod. Phys. **83**, 1057 (2011).
[28] R. Qi, X.L. Yu, Z.B. Li and W.M. Liu, *Non-Abelian Josephson effect between two F=2 spinor Bose-Einstein condensates in double optical traps*, Phys. Rev. Lett. **102**, 185301 (2009).
[29] J. Radić, T.A. Sedrakyan, I.B. Spielman, and V. Galitski, *Vortices in spin-orbit-coupled Bose-Einstein condensates*, Phys. Rev. A **84**, 063604 (2011).
[30] J.B. Rosen, *The gradient projection method for nonlinear programming, Part I: Linear constraints*, SIAM J. Appl. Math. **8**, 181-217 (1960).
[31] J.B. Rosen, *The gradient projection method for nonlinear programming, Part II. Nonlinear constraints*, SIAM J. Appl. Math. **9**, 514-532 (1961).
[32] J. Ruseckas, G. Juzeliūnas, P. Ohberg and M. Fleischhauer, *Non-Abelian gauge potentials for ultracold atoms with degenerate dark states*, Phys. Rev. Lett. **95**, 010404 (2005).
[33] E. Ruokokoski, J.A.M. Huhtamäki and M. Möttönen, *Stationary states of trapped spin-orbit-coupled Bose-Einstein condensates*, Phys. Rev. A **86**, 051607 (2012).
[34] H. Sigurdsson, T.C.H. Liew, O. Kyriienko and I.A. Shelykh, *Vortices in spinor cold exciton condensates with spin-orbit interaction*, Phys. Rev. B **89**, 035302 (2014).
[35] S. Sinha, R. Nath and L. Santos, *Trapped two-dimensional condensates with synthetic spin-orbit coupling*, Phys. Rev. Lett. **107**, 270401 (2011).

[36] S. Song, D. Wang, H. Wang and W.M. Liu, *Generation of ring dark solitons by phase engineering and their oscillations in spin-1 Bose-Einstein condensates*, Phys. Rev. A **85**, 063617 (2012).

[37] S. Song, Y. Zhang, L. Wen and H. Wang, *Spin-orbit coupling induced displacement and hidden spin textures in spin-1 Bose-Einstein condensates*, J. Phys. B: At. Mol. Opt. Phys. **46**, 145304 (2013).

[38] T.D. Stanescu, C. Zhang and V.M. Galitski, *Non-equilibrium spin dynamics in a trapped Fermi gas with effective spin-orbit interaction*, Phys. Rev. Lett. **99**, 110403 (2007).

[39] T.D. Stanescu, B. Anderson and V. Galitski, *Spin-orbit coupled Bose-Einstein condensates*, Phys. Rev. A **78**, 023616 (2008).

[40] H. Wang, *Numerical simulation on stationary states for rotating two-component Bose-Einstein condensates*, J. Sci. Comput. **38**, 149-163 (2009).

[41] H. Wang, *A projection gradient method for computing ground state of spin-2 Bose-Einstein condensates*, J. Comput. Phys. **274**, 473-488 (2014).

[42] H. Wang and Z. Xu, *Projection gradient method for energy functional minimization with a constraint and its application to computing the ground state of spin-orbit-coupled Bose-Einstein condensates*, Comput. Phys. Commun. **185**, 2803-2808 (2014).

[43] C. Wang, C. Gao, C. Jian and H. Zhai, *Spin-orbit coupled spinor Bose-Einstein condensates*, Phys. Rev. Lett. **105**, 160403 (2010).

[44] L. Wen, Q. Sun, H.Q. Wang, A.C. Ji and W.M. Liu, *Ground state of spin-1 Bose-Einstein condensates with spin-orbit coupling in a Zeeman field*, Phys. Rev. A **86**, 043602 (2012).

[45] F. Wilczek, *Majorana returns*, Nat. Phys. **5**, 614-618 (2009).

[46] Z.F. Xu, Y. Kawaguchi, L. You and M. Ueda, *Symmetry classification of spin-orbit coupled spinor Bose-Einstein condensates*, Phys. Rev. A **86**, 033628 (2012).

[47] H. Zhai, *Spin-orbit coupled quantum gases*, Int. J. Mod. Phys. B **26**, 1230001 (2012).

[48] X. Zhang, B. Li and S. Zhang, *Rotating spin-orbit coupled Bose-Einstein condensates in concentrically coupled annular traps*, Laser Phys. **23** 105501 (2013).

[49] Y. Zhang, M. Mossman, T. Busch, P. Engels and C. Zhang, *Properties of spin-orbit-coupled Bose-Einstein condensates*, Front. Phys. **11**, 118103 (2016).

[50] Y. Zhang, L. Mao and C. Zhang, *Mean-field dynamics of spin-orbit coupled Bose-Einstein condensates*, Phys. Rev. Lett. **108**, 035302 (2012).